Organic Farming
https://www.acadlore.com/journals/OF

Rainfall Forecasting in Central Lombok Using an Enhanced Facebook Prophet Model with Multiplicative Seasonality

Yuyun Hidayat[1*], Budhi Handoko[1], Yosefina Pradjanata[2]

[1] Department of Statistics, Padjadjaran University, 45363 Jatinangor, Indonesia
[2] Bachelor Degree Program of Statistics Department, Padjadjaran University, 45363 Jatinangor, Indonesia

[*] Correspondence: Yuyun Hidayat (yuyun.hidayat@unpad.ac.id)

Received: 03-20-2025 **Revised:** 06-23-2025 **Accepted:** 07-05-2025

Citation: Hidayat, Y., Handoko, B., & Pradjanata, Y. (2025). Rainfall forecasting in central Lombok using an enhanced Facebook Prophet model with multiplicative seasonality. *Org. Farming*, *11*(3), 173–184. https://doi.org/10.56578/of110303.

Abstract: Accurate rainfall forecasting remains critical for climate-sensitive agricultural planning, particularly in monsoon-driven regions where rice production is highly vulnerable to hydrometeorological variability. In this study, rainfall in Central Lombok Regency was forecasted using an enhanced version of the Facebook Prophet model incorporating a multiplicative seasonal component. Univariate monthly rainfall data (measured in millimeters) from January 1991 to July 2024 were utilized to train and evaluate the model. A configuration yielding optimal performance produced a Mean Absolute Percentage Error (MAPE) of 18.08% on the testing set, with 80.19% of the forecasted values exhibiting an Absolute Percentage Error (APE) below 20%, indicating a high level of predictive reliability. Forecasting was conducted over a short-term horizon of nine 10-day periods (approximately three months). Analysis of the forecast outputs identified the transition period from the dry to the rainy season—early August to late October—as the most favorable window for initiating rice planting. By aligning planting schedules with anticipated rainfall patterns, the likelihood of crop failure can be mitigated, thereby enhancing productivity and supporting local food security. The findings underscore the practical utility of interpretable time series models in developing data-driven agricultural calendars and advancing climate-resilient farming practices. This approach is particularly relevant for tropical monsoon regions facing increasingly erratic rainfall due to climate change. Furthermore, the demonstrated integration of seasonality effects within the Prophet framework contributes methodologically to the broader field of agro-meteorological forecasting.

Keywords: Rainfall forecasting; Climate variability; Facebook Prophet; Multiplicative seasonality; Rice cultivation; Agricultural risk; Central Lombok

1. Introduction

1.1 Background

The province of West Nusa Tenggara is known as one of the main food producers in Indonesia, with high rice production. Based on the data from the Central Statistics Agency (Badan Pusat Statistik [BPS-Statistics Indonesia], 2023), the province ranks 8th nationally, with a total production reaching 1,538,536.92 tons. However, failures often occur due to drought caused by low rainfall or, conversely, damage due to intense storm rains. This condition makes rice, a commodity, highly sensitive to weather fluctuations, requiring more attention in water resource management and planting strategies. Central Lombok Regency has become one of the main agricultural areas in the province, heavily relying on rainfall patterns to support its agricultural productivity. Although the region has a functioning irrigation system, dependence on rainfall remains high, especially in areas without full irrigation coverage. Significant fluctuations in rainfall, whether drought or heavy rain, can directly impact yields, cause flooding, or erode topsoil. Efficient water management and climate change adaptation strategies are thus crucial.

In 2021-2024, there were several prediction errors that caused losses to farmers. For example, when the Meteorology, Climatology, and Geophysics Agency (BMKG) predicted the start of the dry season, heavy rains followed, flooding newly planted rice fields. Similarly, forecasts of the rainy season sometimes preceded periods of unexpected drought, harming crops near harvest time. These inaccuracies are partly due to the complex and dynamic nature of the atmosphere, making weather predictions inherently uncertain. Forecasting rainfall is one of the primary tools to reduce agricultural risk. Various models such as Autoregressive Integrated Moving Average (ARIMA), Long Short-Term Memory (LSTM), and hybrid approaches have been employed for this purpose. However, these methods often demand extensive tuning, are sensitive to missing data, or do not perform well with outliers. The Facebook Prophet model, introduced by Taylor & Letham (2018), offers a flexible approach capable of handling trend shifts, strong seasonality, missing values, and outliers.

Although Prophet is widely used in finance and business, its application in weather-and climate-related forecasting is emerging. For example, Toharudin et al. (2021) used Prophet for air temperature forecasting, while Zhao et al. (2018) applied it to $PM_{2.5}$ pollution levels. In the rainfall domain, Ruswanti (2020) compared Prophet with Neural Networks (NN) and Support Vector Machines (SVM), showing competitive accuracy. However, there is still a lack of comparative literature that evaluates Prophet specifically for rainfall prediction in tropical monsoon regions like Indonesia. This research addresses that gap by applying Prophet to long-term, high-frequency rainfall data from Central Lombok and comparing the model's accuracy using Mean Absolute Percentage Error (MAPE) and Absolute Percentage Error (APE) (Aldrian et al., 2011).

Figure 1 illustrates long-term rainfall variability over time, highlighting clear seasonal trends (repeating annual cycles) and interannual differences (year-to-year fluctuations). Several extreme events (e.g., high rainfall spikes and dry spells) are also visible. Based on Figure 1, it can be seen that the rainfall in Central Lombok Regency fluctuates significantly each year, or it can be said to have high variability. In addition, there are several extreme data points marked by very high or low data. In the plot, a clear seasonal pattern is also visible. Based on the visuals, it is indicated that the seasonal pattern is multiplicative. This is marked by an unstable seasonal pattern over time, but it is confirmed again in section 2.1.

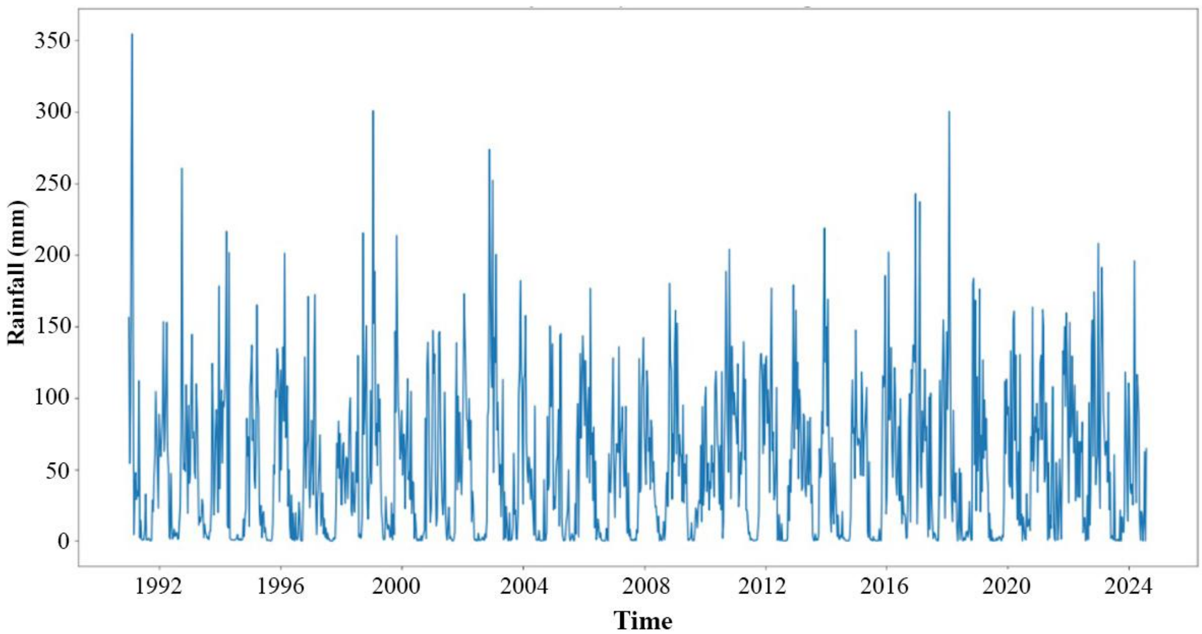

Figure 1. Rainfall plot for Central Lombok Regency, West Nusa Tenggara Province (January 1991-July 2024)
Source: BMKG Verification Book, processed by authors.

1.2 Problem Identification

Unpredictable rainfall in Central Lombok Regency poses a significant challenge to the agricultural sector, especially in rice food production. Errors in predicting rainfall can have a negative impact on agricultural activities. Error in prediction means that there is a chance that the prediction made will be an overestimate or underestimate. Both of these conditions can harm farmers by causing low harvest and poor crop quality. If the prediction is overestimated, the crops may experience drought and the farmers will not have enough time to prepare excess water, whereas if the prediction is underestimated, the farmers will not have enough time to devise a strategy in case of flooding.

1.3 Research Objective

This study aims to find a suitable model to forecast rainfall data in Central Lombok Regency for the upcoming decades. In addition, this study aims to obtain more accurate rainfall forecasting results for Central Lombok Regency over the next few decades using the selected model.

1.4 Scope and Limitations

This research uses secondary data from BMKG. The data obtained is rainfall data in Central Lombok Regency for the period from January 1991 to July 2024, consisting of 1,209 observation units. In addition, the historical data used in this study is univariate time series data or data with one variable.

2. Methodology

2.1 Data Source

The data used in this research are secondary data related to rainfall in millimeters from January 1991 to July 2024, with a total of 1,209 observation units. The variable used is only one independent variable. Rainfall has two categories: rainfall above 1 mm is interpreted as rain, while rainfall below 1 mm is interpreted as no rain.

Based on Figure 1, it can be observed that the plot has six characteristics that have already been proven by tests. The characteristics are high variability (proven by the control chart where there are a lot of data outside the upper control limit line), multiplicative seasonality (proven by the autocorrelation function where the seasonality plot gets smaller from lag 1 until lag 1000), outliers (proven by the boxplot where there are few data outside the boxplot), autocorrelation (proven by the run test), nonlinearity (proven by the Ramsey RESET test), and trend (proven by the Cox-Stuart test).

2.2 Data Analysis

The Facebook Prophet model was used as the forecasting model in this research. The model treats time series forecasting as a curve-fitting exercise without considering the temporal dependency structure in the underlying data (Malefors et al., 2021). This model has advantages compared to several other models because of its ability to accommodate multiple period seasonality, handle all types of trends, and adjust the degree of smoothness. The Facebook Prophet model produces good results even in the presence of missing data, long trends, or many outliers in the dataset.

The Facebook Prophet model algorithm falls under the semi-automatic forecast category, where there is a division of tasks between humans and machines within this model (Žunić et al., 2020). This division of tasks is explained in Figure 2.

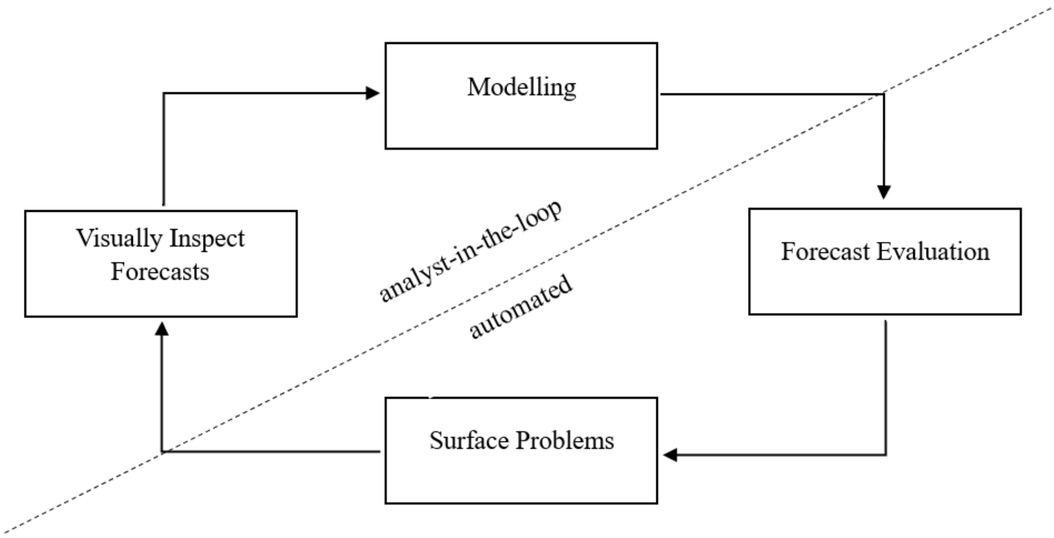

Figure 2. Scheme of the Facebook Prophet model

In the Facebook Prophet model, the forecasting process begins with data visualization as a form of representation in the subsequent model formation. The second process is model formation through hyperparameter tuning of trend, seasonal, holiday, and other component parameters. The next step is to evaluate the performance of the model. If the model's performance is not yet satisfactory, the model-building process can be repeated until optimal results are achieved. The final process involves addressing any issues that arise in the forecasting results, allowing the authors to intervene, analyze the outcomes, and modify the model as necessary (Toharudin et al., 2021).

Facebook Prophet is one of the time series forecasting methods developed by Facebook's Core Data Science team. This method consists of three main components: trend, seasonal, and holiday functions. The trend function is to model non-periodic changes in time series data. The seasonal function is to represent periodic changes (e.g., daily, weekly, dekad, biweekly, monthly, and yearly). The holiday function is to represent the effects of holidays that occur on an irregular schedule over one or several days. This method is very effective in handling trend shifts, fluctuating data, strong seasonality, and outliers. The general equation of Facebook Prophet is in Eq. (1):

$$Y(t) = g(t) + s(t) + h(t) + \varepsilon \tag{1}$$

where, $Y(t)$ is the observation value at time t; $g(t)$ is the trend function that represents long-term changes in the data; $h(t)$ is the holiday function, which captures the impact of special events such as national holidays or other occurrences that repeat irregularly; $s(t)$ is the seasonal function, which represents periodic patterns in the data; and ε is the error or residual noise, which is assumed to be white noise with a normal distribution, $\varepsilon \sim N(0,\sigma^2)$.

Because the seasonal pattern in this study is multiplicative, there is a modification to the general equation (Borges & Nascimento, 2022). The equation for the multiplicative seasonal pattern is as follows (Ensafi et al., 2022):

$$Y(t) = (g(t) + h(t)) \times (1 + s(t)) + \varepsilon \tag{2}$$

The trend function is calculated using a piecewise linear or logistic growth model, which can adjust to changes in trend patterns with changepoints. Because this model is multiplicative, the seasonal effect is modeled as a proportion of the underlying trend (Bee Dagum, 2010).

2.2.1 Trend function

The growth component aims to understand how the data population is developing. This component is made as similar as possible to the factual one. Growth is usually modeled using the logistic growth model in its most basic form as follows (Subashini et al., 2019):

$$g(t) = \frac{C}{1 + \exp(-k(t - m))} \tag{3}$$

where, C is the carrying capacity, k is the growth rate, and m is the offset parameter.

There are two issues in using the logistic growth model, namely carrying capacity and non-constant growth rate. To address this, the carrying capacity can be changed to a time-varying capacity, denoted as $C(t)$, and the vector of rate adjustment can be defined as $\delta \in \mathbb{R}^2$, and the vector $a(t) \in \{0,1\}^S$, rate at time t can be defined as $k + a(t)^T\delta$, resulting in the following piecewise logistic growth model equation (Upmann et al., 2021):

$$g(t) = \frac{C(t)}{1 + \exp(-(k + a(t)^T \delta)(t - (m + a(t)^T \delta)} \tag{4}$$

Changepoints are moments when the direction of the data changes. For forecasts that do not show saturated growth and a piecewise constant rate of growth, the trend model becomes represented by the following equation (Subashini et al., 2019):

$$g(t) = (k + a(t)^T \delta)t + (m + a(t)^T \gamma) \tag{5}$$

where, $g(t)$ is the trend function that represents the change in value over time t; k is the initial growth rate before any changepoint, which indicates the baseline growth rate of the data before any trend change; m is the offset parameter, which acts as the intercept in the linear regression model and ensures the trend function starts from the appropriate value; δ is the vector of rate adjustments, which contains changes in the slope at each trend changepoint; γ is the vector of intercept adjustments, which ensures the continuity of the trend function after the changepoint; and $a(t)$ is the indicator vector, which shows whether time t has passed a certain turning point, defined as:

$$a_j(t) = \begin{cases} 1, & if\ t \geq s_j\ (passing\ the\ changepoint\ j) \\ 0, & if\ t < s_j \end{cases} \quad (6)$$

Changepoint prior scale is used to adjust the flexibility level of the trend. This aims to address the issues of underfitting and overfitting. This model can be used to determine the time of a trend change (Subashini et al., 2019). When the model is extrapolated beyond the historical data to make predictions, the trend will have constant values. Generative forward models can be used to estimate uncertainty in trend forecasting. Future changepoints can be taken randomly so that the average frequency of changepoints matches the historical data. Thus, the equation becomes as follows (Subashini et al., 2019):

$$\forall_j > T, \begin{cases} \delta_j = 0\ w.p. \dfrac{T-S}{T} \\ \delta_j \sim Laplace(0, \lambda) w.p. \dfrac{S}{t} \end{cases} \quad (7)$$

2.2.2 Seasonal function

In time series data, seasonal patterns with multiple periods are often found. For example, the dry season and the rainy season in several months repeat every year (Harvey & Shephard, 1993). To adjust and forecast these effects, a periodic function of t is needed to determine the seasonal component. Fourier series are used in this prophet model to provide a more flexible model of periodic effects, with P being the expected regular period. Thus, the arbitrary smooth seasonal effect becomes as follows (Taylor & Letham, 2018):

$$s(t) = \sum_{n=1}^{N} \left(a_n \cos\left(\frac{2\pi t}{P}\right) + b_n \sin\left(\frac{2\pi t}{P}\right) \right) \quad (8)$$

where, $\beta=[a_{1,}, b_1, \ldots, a_n, b_n]^T$.

$$a_n = \frac{1}{P} \int_{-P}^{P} f(x) \cos\left(\frac{2\pi nt}{P}\right) dx \quad (9)$$

$$b_n = \frac{1}{P} \int_{-P}^{P} f(x) \sin\left(\frac{2\pi nt}{P}\right) dx \quad (10)$$

where, n = 1, 2..., N means that the seasonal pattern is represented as a combination of several harmonics; N is the number of waves; P is the 10-day period (e.g., if yearly, then P = 365; if weekly, then P = 7); a_n and b_n are the Fourier coefficients that regulate the amplitude (contribution) of each cosine and sine signal at the n^{th} harmonic level, whose values are estimated from historical data; *cos* is the cosine function that captures seasonal changes in a symmetric form (starting from a peak or minimum value); and *sin* is the sine function that captures an asymmetric seasonal pattern (starting from 0) (Haqiqatkhah & Hamaker, 2025).

2.2.3 Modified holiday function

Although rainfall data does not naturally include holidays, the holiday component of the Prophet model in this study was creatively modified to reflect unexpected rainfall anomalies—effectively treating certain deviations as "pseudo-holidays" that disrupt the usual seasonal pattern. This innovation allows the model to capture sudden rainfall shifts that might affect agricultural planning.

Specifically, a "modified holiday" is defined when:

(1) Rainfall is less than 1 mm during a period that is statistically classified as the rainy season (expected ≥ 1 mm);

(2) Rainfall is greater than or equal to 1 mm during a period that falls within the dry season (expected < 1 mm).

The following is the equation used to calculate the contribution of holidays to the model (Taylor & Letham, 2018):

$$z(t) = [1(t \in D_1), \ldots, (t \in D_L)] \quad (11)$$

$$h(t) = z(t)k \quad (12)$$

where, $z(t)$ is the holiday indicator matrix, where each element indicates whether time t falls within a certain set of holidays. If t falls on a holiday, then the element in the vector $z(t)$ will be 1; otherwise, it will be 0. In addition, $k \sim Normal\,(0,v^2)$ is the vector of holiday effect that follows a normal distribution with a mean of 0 and variance; and $h(t)$ is the total holiday effect generated from the multiplication of the indicator matrix $z(t)$ with the holiday effect k.

These deviations often indicate short-term climate anomalies, such as false starts or abrupt transitions between seasons. By tagging these points as holidays, the model can adjust predictions to account for irregular events not explained by regular trend or seasonal components (Li et al., 2022). This interpretation strengthens the model's ability to flag and adapt to extreme rainfall behavior—an important capability for practical farming decisions in tropical monsoon regions (Kalyan, 2024).

2.3 Conceptual Design

Figure 3 shows the conceptual design of this study.

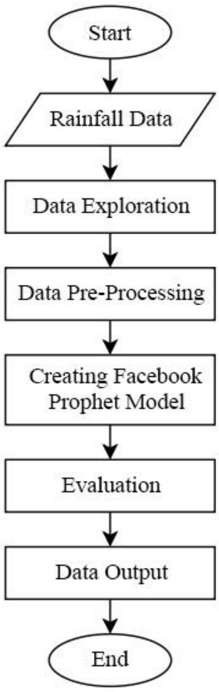

Figure 3. Conceptual design of the research

2.4 Parameters

Seven parameters were used in this research. Interval width is used to determine the width of the confidence interval for predictions. The default value is 0.8, or an 80% confidence interval. Seasonality mode is used to determine whether the seasonal component is additive or multiplicative. Because the data used in this study is multiplicative, the seasonality mode used is "multiplicative". Holidays are used for the holiday list. Changepoint prior scale is used to control the model's sensitivity to trend changepoints. If it is larger, the model becomes more flexible in capturing trend changes. Seasonality prior scale is used to control the strength of regularization for the seasonal component. If it increases, the model becomes more flexible in capturing seasonal patterns. Holiday prior scale is used to control the strength of regularization on holiday effects. If it increases, it allows for a more varied holiday effect. And Fourier series is used to determine the number of Fourier components used in the seasonal model. If it increases, the model becomes more complex, capturing finer details of seasonal patterns (Sulaiman et al., 2023).

2.5 Evaluation Metrics

APE was used to evaluate the first model in this research. It calculates the magnitude of the error for each individual observation value. Just like MAPE, if the error value decreases, the accuracy level increases. The smaller the APE value, the smaller the MAPE value because MAPE is the average of all APE values (Chang et al., 2007).

$$APE = \left|\frac{X_t - \hat{X}_t}{X_t}\right| \times 100\% \quad (13)$$

where, X_t is the observed value, and $\hat{X}_t$ is the predicted value. The smaller the APE value, the better.

MAPE was used to evaluate the second model in this study. It is a method of measuring error in forecasting methods using the absolute error technique in each period divided by the actual observation value for that period (Candra et al., 2018). After that, calculations were performed to obtain the average APE. MAPE is an error test that can measure the percentage difference between predicted and actual data. The following is the equation for MAPE calculation:

$$MAPE = \frac{1}{n}\sum_{t=1}^{n}\left|\frac{X_t - \hat{X}_t}{X_t}\right| \times 100\% \quad (14)$$

where, X_t is the observed value, and $\hat{X}_t$ is the predicted value.

3. Results

3.1 Selected Model

As for 1,209 data points, computer assistance is needed to involve all the existing data. The parameters that were not changed during hyperparameter tuning include interval width (IW), seasonality mode (SM), and holidays (H). Meanwhile, the parameters changed during the tuning include changepoint prior scale (CPS), seasonality prior scale (SPS), holidays prior scale (HPS), and fourier order (FO).

Based on Table 1, the model with the best training and testing accuracy were chosen because high accuracy means that the model can follow the existing rainfall data patterns. Thus, the bold data in Table 1 shows the final combination of the selected Facebook Prophet model. Then the best combination of parameter that will be use is combination of CPS = 0.1, SPS = 15, HPS = 15 and FO = 6, this combination gave lowest MAPE train (16.26%) and MAPE test (18.08%).

Table 1. Parameter combinations

Prior Scale (CPS)	Seasonality Prior Scale (SPS)	Holidays Prior Scale (HPS)	Fourier Order (FO)	MAPE Train (%)	MAPE Test (%)
0.05	10	10	4	32.79	31.52
0.05	10	10	6	42.92	23.07
0.05	10	10	8	42.37	25.17
0.05	10	15	4	32.98	32.33
0.05	10	15	6	33.68	22.18
0.05	10	15	8	42.19	25.13
0.05	10	20	4	33.45	32.96
0.05	10	20	6	33.73	23.16
0.05	10	20	8	42.29	25.10
0.05	12	10	4	33.53	33.03
0.05	12	10	6	33.12	22.65
0.05	12	10	8	42.14	25.23
0.05	12	15	4	32.94	31.97
0.05	12	15	6	32.75	21.99
0.05	12	15	8	42.16	25.26
0.05	12	20	4	33.14	32.15
0.05	12	20	6	33.28	23.09
0.05	12	20	8	41.94	24.19
0.05	15	10	4	32.55	31.42
0.05	15	10	6	32.37	21.73
0.05	15	10	8	42.33	25.90
0.05	15	15	4	32.89	31.96
0.05	15	15	6	33.82	23.26
0.05	15	15	8	42.53	26.18
0.05	15	20	4	33.44	32.45
0.05	15	20	6	32.74	22.19
0.05	15	20	8	42.26	24.89
0.1	10	10	4	19.28	21.90

0.1	10	10	6	20.82	23.97
0.1	10	10	8	28.87	30.15
0.1	10	15	4	23.44	26.96
0.1	10	15	6	19.79	23.97
0.1	10	15	8	24.34	25.15
0.1	10	20	4	21.85	23.68
0.1	10	20	6	20.79	24.19
0.1	10	20	8	27.35	23.75
0.1	12	10	4	30.73	32.88
0.1	12	10	6	18.14	22.20
0.1	12	10	8	19.54	20.24
0.1	12	15	4	21.65	24.18
0.1	12	15	6	18.77	20.76
0.1	12	15	8	25.83	33.59
0.1	12	20	4	19.55	18.24
0.1	12	20	6	25.77	26.76
0.1	12	20	8	22.45	18.24
0.1	15	10	4	18.00	20.14
0.1	15	10	6	16.99	19.19
0.1	15	10	8	22.39	24.45
0.1	15	15	4	21.66	23.90
0.1	**15**	**15**	**6**	**16.26**	**18.08**
0.1	15	15	8	20.96	24.78
0.1	15	20	4	22.62	23.91
0.1	15	20	6	17.12	19.92
0.1	15	20	8	18.01	20.58

The following is the mathematical equation of the selected Facebook Prophet model:

$$Y(t) = ((0.00498 + a(t)^T\delta)t + (4.0731 + a(t)^T\gamma) + z(t)0.466) \times (1 + s(t)) \quad (15)$$

The interpretation of the model above is that the trend growth is 0.00498, the intercept is 4.0731, and the contribution indicator vector for holidays is 0.466. $a(t)^T$ produces values of 1 and 0, depending on whether time t has passed the changepoint or not. δ is the rate adjustment or slope change. Since there are many changepoints, the rate adjustment depends on which changepoint the time point follows. γ is the intercept adjustment, or change in intercept. Because there are many changepoints, the intercept adjustment is determined by the changepoint most recently passed by the time point. $s(t)$ is obtained from the coefficients *an* and *bn*, which are calculated at their respective harmonics. $z(t)$ contains 1 and 0, depending on whether the data is a holiday or not.

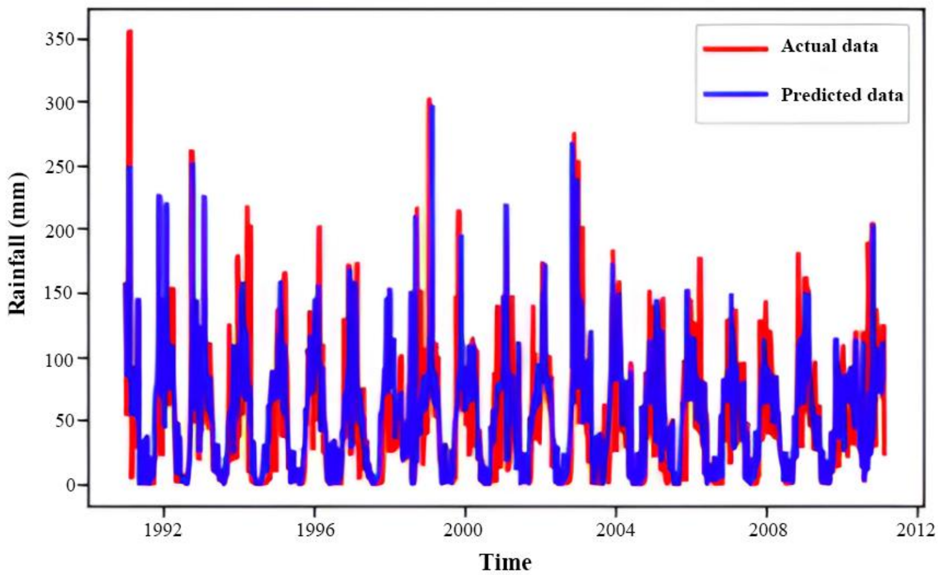

Figure 4. Comparison between actual and predicted rainfall data (training) from 1992 to 2012

Comparison between actual and predicted data using the training data is showed in Figure 4. Based on Figure 4, it can be seen that the model can follow the pattern of actual data, although not all of it is the same. But in accordance with the statement that Facebook Prophet can handle extreme data, this is proven in the results, as the model can follow extreme data even though it does not perfectly match all data points. Seasonal patterns are also clearly formed and are the same as the actual data. In addition to viewing the graph, it can also be seen in detail through the comparison results in Table 2.

From Table 2, the Average Percentage Error (APE) of all training data was tested. It was found that 82.11% of the training data have an APE value below 20%. Meanwhile, the remaining 17.89% of the training data have an APE value above 20%. Afterwards, to ensure that the model is not overfitting, another comparison was conducted using the testing data.

Table 2. Comparison results between actual and predicted rainfall data (training) from January 1991 to February 2011

Date	Actual Rainfall (mm)	Prediction Rainfall (mm)	APE (%)
1991-01-01	156.2082	164.3923954	5.239286654
1991-01-02	54.2188	63.39059107	16.91625612
1991-01-03	96.4405	95.85044027	0.611838105
1991-02-01	272.4702	284.0455986	4.248317283
…	…	…	…
2011-01-02	81.7819	88.69367526	8.45147308
2011-01-03	67.9422	75.28388185	10.80577586
2011-02-01	123.7731	114.7916442	7.256387547
2011-02-02	23.9576	31.42686024	31.17699701

Based on Figure 5, it can be seen that the model can follow the actual testing data, although not exactly the same. In addition, the details can also be seen through the comparison results in Table 3.

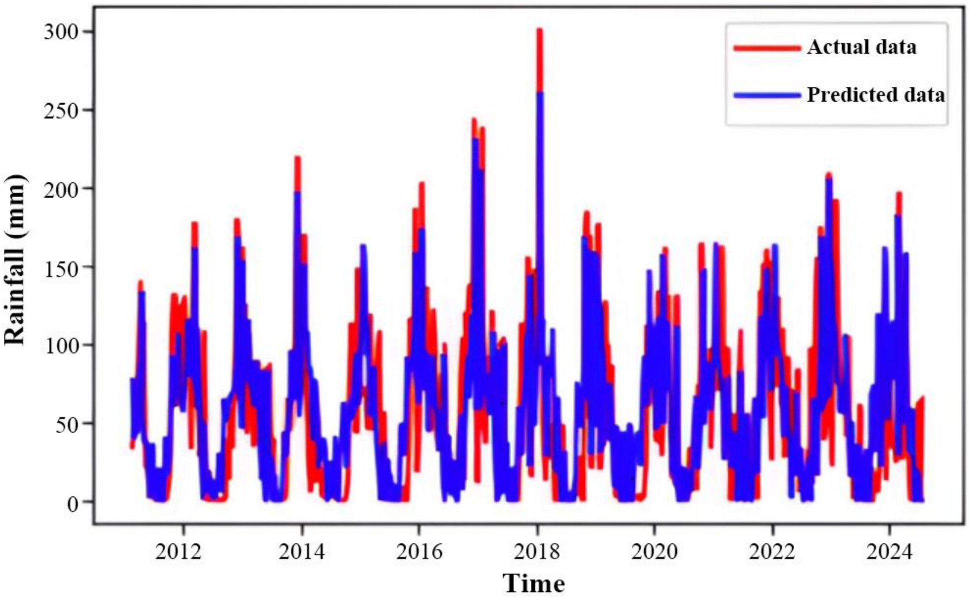

Figure 5. Comparison between actual and predicted rainfall data (testing) from 2012 to 2024

Table 3. Comparison results between actual and predicted rainfall data (testing) from February 2011 to July 2024

Date	Actual Rainfall (mm)	Prediction Rainfall (mm)	APE (%)
2011-02-03	34.163	37.27855993	9.119690691
2011-03-01	61.9639	54.63696647	11.82451965
2011-03-02	46.8193	53.66281828	14.61687441
2011-03-03	67.6593	60.44190968	10.66725539
…	…	…	…
2024-06-03	12.4904	14.13214497	13.14405443
2024-07-01	62.3358	60.87290453	2.346798252
2024-07-02	0.11308	0.13451891	18.95906475
2024-07-03	64.5396	55.28082078	14.34588876

From Table 3, the APE of all testing data was tested. It was found that 80.19% of the testing data have an APE value below 20%. Meanwhile, the remaining 19.81% of the testing data have an APE value above 20%. Because the model proved capable of following the rainfall pattern during training and testing, and its accuracy was also quite high, the model was selected as the one to be used for future rainfall data predictions.

3.2 Prediction

After obtaining the best model, it was used to predict rainfall for the next nine 10-day periods (three months ahead). Figure 6 and Table 4 show the results of the prediction. Based on Figure 6, it can be seen that the rainfall is quite high as the rainy season is approaching.

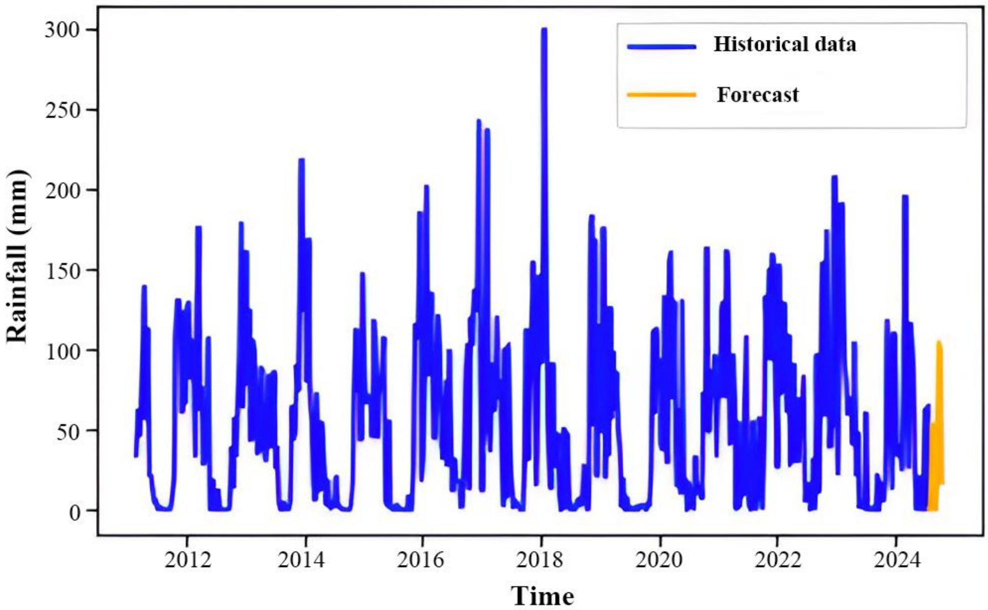

Figure 6. Prediction of rainfall in 2024

Table 4. Rainfall prediction results during August to October, 2024

Date	Rainfall Prediction (mm)
2024-08-01	1.208
2024-08-02	48.3860
2024-08-03	0.4266
2024-09-01	47.78839
2024-09-02	10.2277
2024-09-03	15.9921
2024-10-01	37.266
2024-10-02	55.4151
2024-10-03	101.873

4. Discussion

The results of this study indicate that the Facebook Prophet method is capable of capturing seasonal patterns and trends in rainfall data in Central Lombok Regency quite well. This model produces relatively accurate predictions compared to the actual values, as shown by the evaluation metrics (APE and MAPE). Facebook Prophet uses a multiplicative approach with trend, seasonal, and modified holiday components to model time series data. In this study, the model successfully identified a consistent seasonal pattern with the climatic characteristics of Central Lombok, where peak rainfall often occurs from September to April and the dry season lasts from May to August.

The findings of this research have important implications for agricultural planning and hydrometeorological disaster mitigation in Central Lombok Regency. With more accurate rainfall predictions, farmers can optimize their planting schedules, while local governments can better anticipate the risks of floods or droughts.

However, this study has several limitations. The Facebook Prophet model used is based solely on historical rainfall data without considering external factors such as the El Niño–Southern Oscillation (ENSO) phenomenon or long-term climate change.

5. Conclusions

After completing the analysis and calculations in the above chapters, several points related to the core of this study can be concluded. The selected Facebook Prophet model has a testing MAPE of 18.078%, with 80.19% of the total data having an APE value below 20%. In addition, prediction data for the next nine 10-day periods has been obtained using the selected model. This study provides several recommendations to the farmers. The best time to plant rice is during the transition from the dry season to the rainy season. Farmers should plant in the first 10-day period of August, and then the rice can be harvested after 90 days, which is in the third 10-day period of October. During this period, there is rain but not extreme. Therefore, the chances of crop failure are low.

Author Contributions

Conceptualization, Y.H., B.H. and Y.P.; methodology, Y.P.; software, Y.P.; validation, Y.H., B.H. and Y.P.; formal analysis, Y.H., B.H. and Y.P.; investigation, Y.H., B.H. and Y.P.; resources, Y.P.; data curation, Y.H., B.H. and Y.P.; writing—original draft preparation, Y.H., B.H. and Y.P.; writing—review and editing, Y.H., B.H. and Y.P.; visualization, Y.P.; supervision, Y.H. and B.H.; project administration, Y.H. and B.H.; funding acquisition, Y.H. and B.H. All authors have read and agreed to the published version of the manuscript.

Funding

The paper was funded by Directorate of Research and Community Engagement of Padjadjaran University.

Data Availability

The actual and predicted rainfall data supporting our research results are available in the Google Drive: https://drive.google.com/drive/folders/150yHiiqg2MP9eI6UdC15BmmzmDkRuu7d?usp=drive_link.

Conflicts of Interest

The authors declare that there are no conflicts of interest related to this research. Although the data taken from Badan Pusat Statistik [BPS-Statistics Indonesia] (2023) and BMKG which are government agencies, does not make the author subjective to the analysis and interpretation of the results. All data sources, literature, and references used have been appropriately acknowledged and no violation of publication ethics has been committed.

References

Aldrian, E., Karmini, M., & Budiman, D. B. (2011). *Adaptation and Mitigation of Climate Change in Indonesia*. Center for Climate Change and Air Quality.

Badan Pusat Statistik [BPS-Statistics Indonesia]. (2023). *Harvest Area, Productivity, and Production of Paddy by Province, 2023*. https://www.bps.go.id/en/statistics-table/2/MTQ5OCMy/luas-panen--produksi--dan-produktivitas-padi-menurut-provinsi.html

Bee Dagum, E. (2010). Time series modeling and decomposition. *Statistica*, *70*(4), 433–457. https://doi.org/10.6092/issn.1973-2201/3597.

Borges, D. & Nascimento, M. C. V. (2022). COVID-19 ICU demand forecasting: A two-stage Prophet-LSTM approach. *Appl. Soft Comput.*, *125*, 109181. https://doi.org/10.1016/j.asoc.2022.109181.

Candra, B. P., Kusrini, & Fatta, H. A. (2018). Implementation of trend moment method for stock prediction as supporting production. *J. Phys. Conf. Ser.*, *1140*, 012031. https://doi.org/10.1088/1742-6596/1140/1/012031.

Chang, P. C., Wang, Y. W., & Liu, C. H. (2007). The development of a weighted evolving fuzzy neural network for PCB sales forecasting. *Expert Syst. Appl.*, *32*(1), 86–96. https://doi.org/10.1016/j.eswa.2005.11.021.

Ensafi, Y., Amin, S. H., Zhang, G., & Shah, B. (2022). Time-series forecasting of seasonal items sales using machine learning–A comparative analysis. *Int. J. Inf. Manag. Data Insights*, *2*(1), 100058. https://doi.org/10.1016/j.jjimei.2022.100058.

Haqiqatkhah, M. M. & Hamaker, E. L. (2025). Daily dynamics and weekly rhythms: A tutorial on seasonal autoregressive-moving average models combined with day-of-the-week effects. *Psychol. Methods*, Advance online publication. https://doi.org/10.1037/met0000756.

Harvey, A. C. & Shephard, N. (1993). Structural time series models. In G. S. Maddala, C. R. Rao, & H. D. Vinod (Eds.), *Handbook of Statistics* (pp. 261-302). Elsevier. https://doi.org/10.1016/S0169-7161(05)80045-8.

Kalyan, N. (2024). *Time series analysis*. BMS College of Engineering.

https://bmsce.ac.in/Content/CDS/Time_Series_Analysis__Unit_1.pdf
Li, J., Li, Z., Wu, H., You, N. (2022). Trend, seasonality, and abrupt change detection method for land surface temperature time-series analysis: Evaluation and improvement. *Remote Sens. Environ.*, *280*, 113222. https://doi.org/10.1016/j.rse.2022.113222.
Malefors, C., Strid, I., Hansson, P. A., & Eriksson, M. (2021). Potential for using guest attendance forecasting in Swedish public catering to reduce overcatering. *Sustain. Prod. Consum.*, *25*, 162–172. https://doi.org/10.1016/j.spc.2020.08.008.
Ruswanti, D. (2020). Pengukuran performa support vector machine dan neural netwok dalam meramalkan tingkat curah hujan. *J. Gaung Informat.*, *13*(1), 66–75.
Subashini, A., Sandhiya, K., Saranya, S., & Harsha, U. (2019). Forecasting website traffic using Prophet time series model. *Int. Res. J. Multidiscip. Technov.*, *1* (1), 56–63. https://doi.org/10.34256/irjmt1917.
Sulaiman, R. B., Hariprasath, G., Dhinakaran, P., & Kose, U. (2023). Time-series forecasting of web traffic using Prophet machine learning model. *FMDB Trans. Sustain. Comput. Lett.*, *1*(3), 161–177.
Taylor, S. J. & Letham, B. (2018). Forecasting at scale. *Am. Stat.*, *72*(1), 37–45. https://doi.org/10.1080/00031305.2017.1380080.
Toharudin, T., Pontoh, R. S., Caraka, R. E., Zahroh, S., Lee, Y., & Chen, R. C. (2021). Employing long short-term memory and Facebook Prophet model in air temperature forecasting. *Commun. Stat. Simul. Comput.*, *52*(2), 279–290. https://doi.org/10.1080/03610918.2020.1854302.
Upmann, T., Uecker, H., Hammann, L., & Blasius, B. (2021). Optimal stock-enhancement of a spatially distributed renewable resource. *J. Econ. Dyn. Control.*, *123*, 104060. https://doi.org/10.1016/j.jedc.2020.104060.
Zhao, N., Liu, Y., Vanos, J. K., & Cao, G. (2018). Day-of-week and seasonal patterns of $PM_{2.5}$ concentrations over the United States: Time-series analyses using the Prophet procedure. *Atmos. Environ.*, *192*, 116–127. https://doi.org/10.1016/j.atmosenv.2018.08.050.
Žunić, E., Korjenić, K, Hodžić, Kerim, & Đonko, D. (2020). Application of Facebook's Prophet algorithm for successful sales forecasting based on real-world data. *Int. J. Comput. Sci. Inf. Technol.*, *12*(2), 23–36. https://doi.org/10.5121/ijcsit.2020.12203.